

Vibrational Characteristics of a Cracked Rotor Subjected to Periodic Auxiliary Axial Excitation

Heba H. El-Mongy, Younes K. Younes and Mohamed S. El-Morsy

Abstract Rotor failure due to cracks can be catastrophic with large costs in down time, damage to equipment and injury to personnel. Prevention of such problems is only attained by developing reliable methods for crack detection and diagnosis. In this paper, the vibratory response of a cracked rotor to an auxiliary axial excitation is investigated experimentally for the purpose of crack detection. An open crack (slot) is artificially created in the rotor-shaft of the experimental rig. The effects of running speed, crack depth and crack-unbalance angle variations on the vibratory response are investigated experimentally. It is shown that the auxiliary excitation method can be efficiently used in crack detection as an online condition monitoring technique. By properly choosing the frequency of the periodic axial excitation and the running speed, the presence of a crack in the excited shaft can be ruled out and the crack growth can be monitored. The crack-unbalance angle can influence the identification process negatively by masking the crack effect on the vibratory response. However, an unbalance trial mass test can help in finding out the unknown crack angle.

Keywords Condition monitoring · Crack detection · Vibration · Auxiliary excitation method

H.H. El-Mongy (✉) · Y.K. Younes · M.S. El-Morsy
Faculty of Engineering, Mechanical Design Department, Mattaria,
Helwan University, P.O. BOX 11718 Cairo, Egypt
e-mail: heba_elmongy@yahoo.com

Y.K. Younes
e-mail: youneskhalil@yahoo.com

M.S. El-Morsy
e-mail: mohsabry1999@yahoo.com

1 Introduction

Cracks in rotating shafts are considered very serious and can lead to catastrophic accidents if not detected in time. There has been extensive research on the vibrational behaviour of cracked shafts and the use of response characteristics to detect cracks. The research in the past few decades on cracked structures and rotors is well documented in review papers [1–5].

Several researchers have identified that a coupling mechanism exists between different types of vibrations, i.e. axial, radial and torsional, in cracked shafts. Such coupling does not appear in absence of a crack. Papadopoulos and Dimarogonas [6–9] have extensively studied coupling of vibration due to crack. They showed that the presence of either of bending, longitudinal or torsional mode natural frequency in the vibration spectra of other modes can be considered a reliable crack indicator. However, they applied sweep excitation to a non-rotating shaft. Ostachowicz and Krawczuk [10] used an open crack model to demonstrate coupling of torsional and bending vibration in a rotating shaft.

Darpe et al. [11] used a non-linear response-dependent breathing crack model to study the coupling of bending and axial vibrations in a slow rotating cracked Jeffcott rotor using periodic axial impulse excitation. Predominant existence of lateral bending natural frequency, axial excitation frequency and side bands around it in lateral vibration spectrum have been shown as important crack indicators. Those analytical results were validated experimentally in [12]. In [13], Darpe et al. numerically studied the coupling between all types of vibrations; longitudinal, lateral and torsional vibrations for a rotating cracked shaft.

It should be noted that simulating a real fatigue crack in a rotating shaft is difficult to attain in a laboratory environment. This is performed as explained by Darpe et al. [14] by introducing an initial slit in the shaft under test then the shaft is placed on a three-point fatigue bending machine where the shaft is subjected to cyclic loading until the crack starts to propagate. In this case, the healthy readings are acquired from the rotor on solid condition, then the system is disassembled and the crack is generated. The system is re-assembled with the cracked shaft and the readings of the faulty condition are acquired. Aside that this procedure is expensive and time costing, it can be difficult to have a valid reference case of the healthy rotor due to misalignment and unbalance that can be introduced during assembly and disassembly [15]. Another disadvantage of this procedure is the possibility of introducing a bow in the rotor. These disadvantages may result in poor comparison between healthy and faulty conditions.

The effect of crack-unbalance angle is also a critical issue in the crack detection process. Early studies by Henry and Okah-Avae [16], Mayes and Davies [17] and Bachschmid et al. [18], indicated that a crack can only affect the synchronous unbalance response if the crack is able to open. This occurs when the unbalance is in phase with the crack where the shaft behaves as a slotted rotor. Similar results were reported for transient response of a cracked rotor as explained by Sawicki et al. [19]. In a detailed numerical and experimental study of the transient response

of a cracked rotor, Darpe et al. [14] showed that the effect of unbalance angle variation depends upon the type of crack whether it is open or breathing which can be used as a diagnostic tool to distinguish both types. To the best of the authors' knowledge, the influence of crack-unbalance angle on the vibration response of a cracked rotor to an external excitation has not been investigated before.

In this paper, the coupling between longitudinal and lateral vibrations due to crack in a rotating shaft is experimentally investigated on a machinery fault demonstrator (PT 500) made by G.U.N.T.[®] An open crack (slot) is artificially created in the rotor-shaft of the test rig. A periodic axial excitation is applied to its rotor in both healthy and cracked conditions. A parametric study is conducted to investigate the effect of crack depth, running speed and crack-unbalance angle on the vibratory response to the applied external axial excitation. Effect of crack-unbalance angle is studied at two different running speeds and two different crack depths in an attempt to thoroughly investigate this interesting effect.

2 Experimental Set-Up

Figure 1 shows a photo and a schematic diagram of the G.U.N.T.[®] machinery fault demonstrator (PT 500) and the measurement and analysis setup located in the Vibration and Dynamics Laboratory of the Faculty of Engineering—Mattaria. The fault demonstrator consists of a steel shaft of diameter 0.02 m and length 0.5 m coupled to an electric motor (0.37 kW) via an elastic spacer ring coupling and supported by two ball bearings (SKF 6004-2ZR). The shaft carries one disc of mass 1.52 kg, diameter 0.15 m and thickness 0.01122 m at mid-span. Figure 1b shows a magnified view of the crack generated in the shaft.

The measurement and analysis setup includes a B&K permanent magnet exciter Type 4808, a B&K power amplifier Type 2712, a B&K exciter control Type 1047, two accelerometers (IMI 603C01) mounted via studs to the BRG#2 (Right bearing) in horizontal and vertical directions, a G.U.N.T.[®] measuring amplifier, a USB bmc[®] data acquisition box and a laptop for data analysis and archiving.

The exciter control is used to generate a sinusoidal signal at the desired frequency. The excitation signal is then amplified by the power amplifier and transferred to the exciter which is positioned horizontally at the shaft end and carefully aligned with the shaft axis.

3 Experimental Approach and Data Analysis

For all the experiments conducted in this study, the vibration signals are acquired at a sampling rate of 8,000 Hz. Number of samples is taken as 64,000 and the time span is 8 s. A LabVIEW[®] virtual instrument is used for data acquisition. The frequency spectra are obtained using National Instruments Sound and Vibration

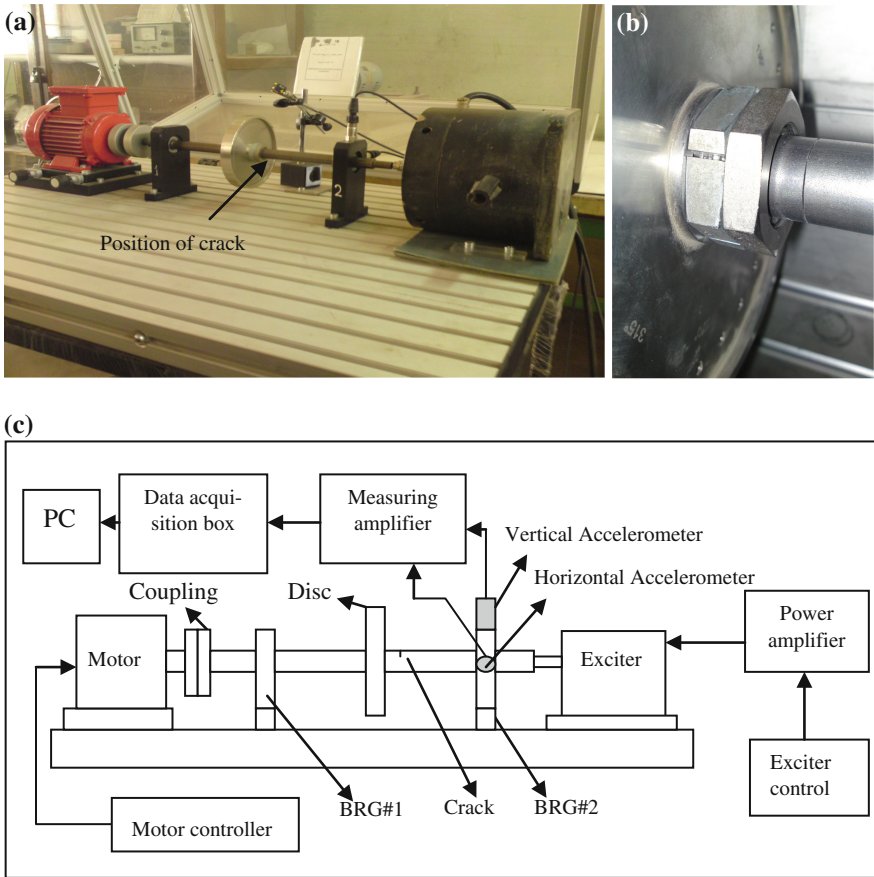


Fig. 1 G.U.N.T.[®] machinery fault demonstrator (PT 500) with measurement and analysis setup, **a** photograph, **b** crack shape, **c** schematic diagram

Assistant[®] software. Power spectrum is chosen for displaying frequency spectra and the vibration parameter is acceleration (RMS).

First, bump test [20] is performed for the shaft under test to find the fundamental bending natural frequency in the horizontal direction. The shaft with the disc situated centrally is suspended using a rope in a “free-free condition” and an accelerometer is fitted to it via magnet. The shaft is hit using an impact hammer and the vibration response is recorded and transformed to the frequency domain. The test is repeated several times to make sure that the results are repeatable and accurate. The fundamental bending natural frequency in the horizontal direction is found to be 313.3 Hz. This frequency is chosen to be the axial excitation frequency for all the experiments as it yields clear frequency spectra [11, 12].

The shaft is then mounted on the fault demonstrator. The machine is allowed to run in for about 4 h before acquiring baseline data for the shaft. Then the crack is created in

the tested shaft at a distance of 5 mm from the taper lock of the disc using a jeweler's saw of width 0.35 mm so the crack is considered as a slot (open crack) as shown in Fig. 1b. The crack depth is increased without need to disassemble the system.

Tests are done at two different crack depths ($\bar{a} = 0.22$) and ($\bar{a} = 0.55$) where \bar{a} defines the relative crack depth ($\bar{a} = a/R$), R is the shaft radius and a is the crack depth. Also, the tests are performed for two different running speeds to investigate the effect of the change of the running speed on the proposed method. The speeds are taken as 1/10th and 1/5th of the first critical speed, i.e., 1,878 and 3,756 RPM respectively.

To investigate the effect of the crack-unbalance angle, an unbalance mass of 3.947 g is placed on the disc at a radius of 60 mm giving eccentricity that equals 0.23682 kg mm. The unbalance mass is first aligned with the crack axis to establish the reference position ($\beta = 0$). The crack-unbalance angle is then varied 25 times in steps of 15° and the lateral vibration in both horizontal and vertical directions is measured for each test case taking into consideration the variation of the crack depth and running speed.

4 Results and Discussion

4.1 Coupling of Lateral and Axial Vibration Due to Crack

Figure 2 represents the frequency spectra of the balanced uncracked shaft without axial excitation where the running speed is taken as 1/10th of the first lateral critical speed of the rotor (1,878 RPM). The 1X component at 31.3 Hz can be seen in the vertical spectrum (Fig. 2b) but in small amplitude because the system is balanced. The bending natural frequency which matches with the 10X harmonic cannot be seen in both horizontal and vertical spectra. Then, axial excitation is applied to the shaft at a frequency equal to the first bending natural frequency ($f_i = 313.3$ Hz). The frequency spectra of the balanced uncracked rotor with axial excitation are shown in Fig. 3. The horizontal spectrum (Fig. 3a) shows the bending natural frequency (f_i) and its first harmonic ($2f_i$), while only ($2f_i$) appears in the vertical spectrum. Ideally, those frequencies should not have appeared because the lateral and axial vibrations are uncoupled in case of uncracked shaft. This could be due to inevitable slight misalignment between the exciter and the rotating shaft which results in coupling between axial and lateral vibrations, i.e. the excitation is not purely axial.

Figure 4 shows the frequency spectra of the cracked shaft ($\bar{a} = 0.22$) without excitation. The horizontal spectrum (Fig. 4a) shows higher harmonics of the 1X including the bending natural frequency (f_i) which matches with the 10X harmonic component. Figure 5 shows the frequency spectra for the cracked shaft with excitation. The bending natural frequency (f_i) and its first harmonic ($2f_i$) are dominant in both spectra (Fig. 5a and b). Compared to Fig. 3a, the amplitude of (f_i) increased from 0.00868 to 0.3708 g^2 and the amplitude of ($2f_i$) increased from 0.00262 to 0.147 g^2 . This increase is only attributed to the crack effect. For such a

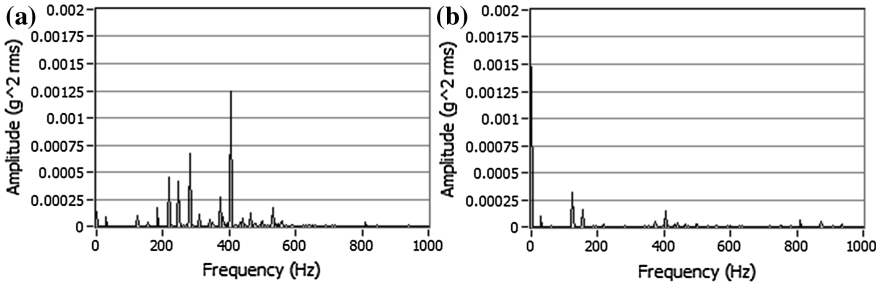


Fig. 2 Frequency spectra of the uncracked shaft without excitation, a horizontal, b vertical

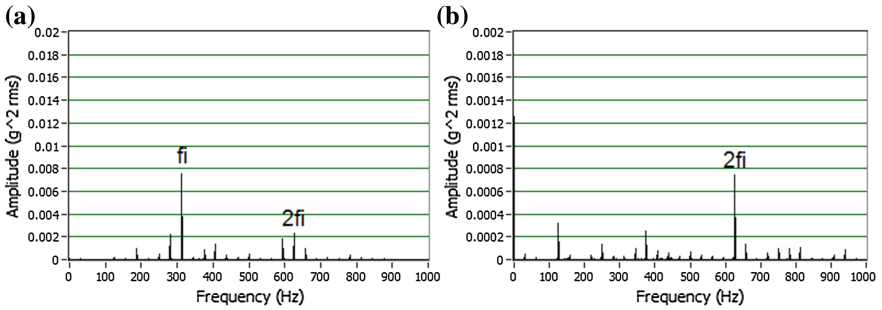


Fig. 3 Frequency spectra of the uncracked shaft with excitation, a horizontal, b vertical

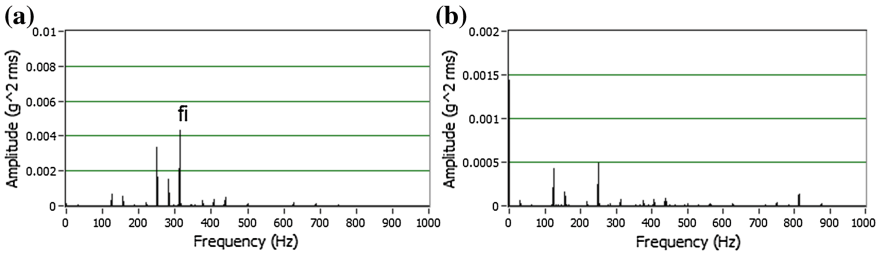


Fig. 4 Frequency spectra of the cracked shaft ($\bar{a} = 0.22$) without excitation, a horizontal, b vertical

small crack depth ($\bar{a} = 0.22$), coupling between lateral and axial vibrations is obviously established. It can be observed that the possible misalignment between the shaft and the exciter is shown to have lower effect on the vibration spectra when compared with the crack effect. Comparing Figs. 2a and 3a, the increase of the (fi) amplitude in the horizontal direction due to misalignment is about 9 times. Meanwhile, the increase of the (fi) amplitude in the horizontal direction due to both the crack effect and the possible misalignment is about 71 times as shown by comparing Figs. 4a and 5a.

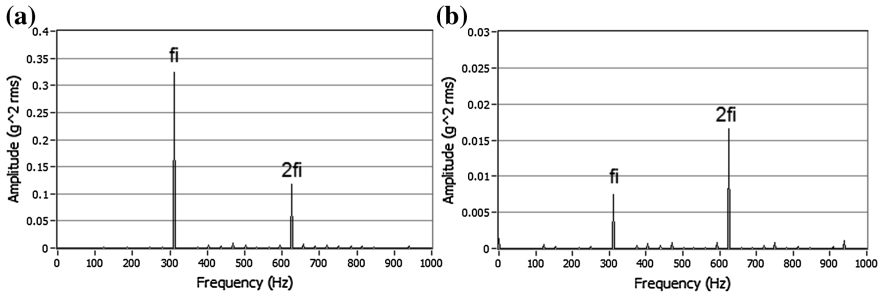


Fig. 5 Frequency spectra of the cracked shaft ($\bar{a} = 0.22$) with excitation, **a** horizontal, **b** vertical

4.2 Parametric Study

4.2.1 Effect of Crack Depth

Figure 6 shows the frequency spectra of the cracked rotor ($\bar{a} = 0.55$) running at speed equal to 1/10th of the first bending natural frequency and excited axially at a frequency equal to the first bending natural frequency (f_i). The patterns of (f_i) and ($2f_i$) can be seen obviously in Fig. 6 as the dominant crack features in the horizontal and vertical spectra. However, the amplitudes of (f_i) and ($2f_i$) are much higher when comparing Figs. 5 and 6. It can be easily inferred from (f_i) and ($2f_i$) amplitude trending that the crack is growing in depth.

4.2.2 Effect of Running Speed

Figure 7 shows the frequency spectra of the unbalanced cracked rotor ($\bar{a} = 0.22$) running at speed equal to 1/5th of the critical speed (3,756 RPM) and subjected to axial excitation at a frequency equal to the first bending natural frequency ($f_i = 313.3$ Hz). The unbalance is placed in phase with the crack. The horizontal

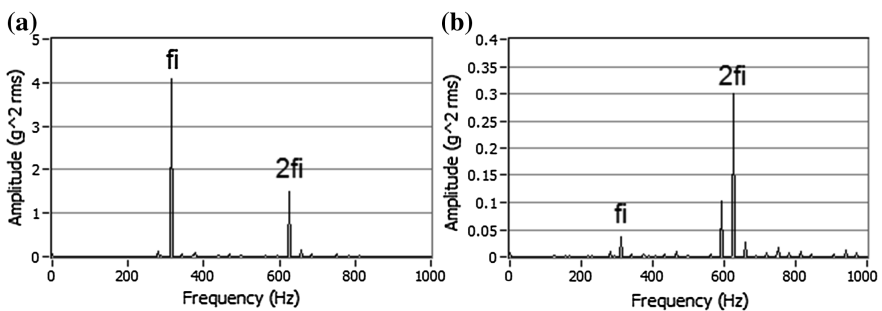


Fig. 6 Frequency spectra of the cracked shaft ($\bar{a} = 0.55$) with excitation, **a** horizontal, **b** vertical

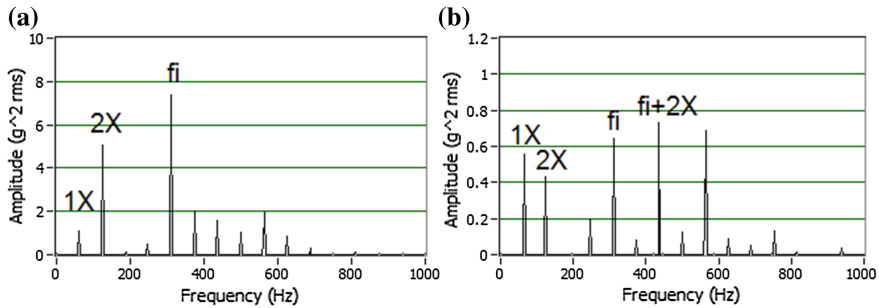


Fig. 7 Frequency spectra of the cracked shaft ($\bar{a} = 0.22$) running at 1/5th of first critical speed with axial excitation at frequency of first bending natural frequency, **a** horizontal, **b** vertical

spectrum (Fig. 7a) shows a high 2X which is the usual symptom of cracked rotors running at a subcritical speed [3, 15]. Also, the (fi) appears as the highest peak in the horizontal spectrum with sum and difference frequencies around it. But they are more obvious in the vertical spectrum (Fig. 7b) where the highest peak is seen at (fi + 2X). These results are in agreement with previous literature [11–13].

4.2.3 Effect of Crack-Unbalance Angle

The measured frequency spectra at different crack-unbalance angles showed similar pattern as the spectra shown in Fig. 5. However, the amplitudes of (fi) and (2fi) varied greatly with the crack-unbalance angle. The variation of the (fi) amplitude for the two crack depth cases is recorded and plotted in Fig. 8. It is obvious from Fig. 8 that the variation pattern of (fi) depends greatly on the crack depth and does not exhibit general behavior. Number of maxima is different in both cases and also the locations of the maxima are shifted. This can be attributed to the fact that increasing the crack depth will result in an increase in the crack angle. This will affect the locations of maxima in the (fi) variation as the regions of crack opening and crack closing will change. The (fi) amplitude for crack depth ($\bar{a} = 0.55$) is generally higher than that for crack depth ($\bar{a} = 0.22$) except in the region of $\beta = 120^\circ:225^\circ$.

For the case of running speed that equals 1/5th of the first critical speed, the same procedure is repeated and the 2X and (fi) are recorded and analyzed. The (fi) amplitude variation (not shown here due to space limitation) is not considered informative because it depends on the running speed and crack depth as shown before in Fig. 8. The 2X variation shown in Fig. 9a was much informative. Inspection of Fig. 9a shows that the 2X amplitude variation resembles a harmonic wave having two cycles with two maxima at $\beta = 0^\circ$ and 105° and two minima at $\beta = 60^\circ$ and 225° . However, in actual situations, unbalance position and crack angle are unknowns. The crack angle can be identified using a test that involves placing trial mass on the rotor and measuring the vibration. The crack angle will lie at one

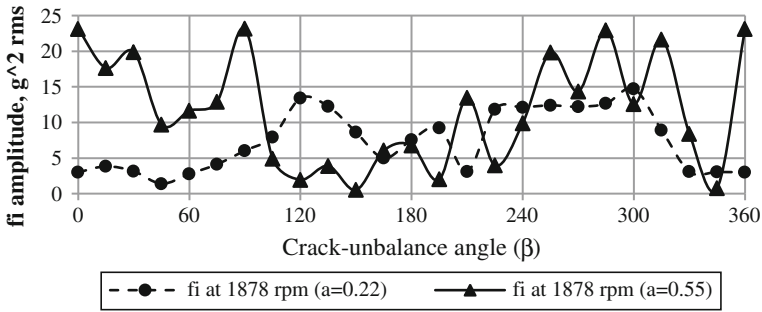


Fig. 8 Variation of amplitude of the horizontal component of first bending natural frequency (f_i) with crack-unbalance angle (β) for different cases of crack depth

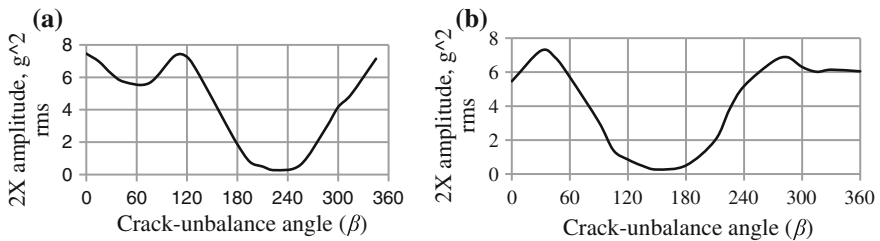


Fig. 9 Variation of amplitude of the horizontal 2X component with crack-unbalance angle (β) for cracked shaft ($\bar{a} = 0.22$) running at 1/5th of its first critical speed, **a** the crack axis is the reference for β , **b** the positive horizontal axis is the reference for β

of the two maxima in the trended results. To prove this observation, the previous test at the same conditions is repeated but the unbalance mass is placed on the disk starting from the positive horizontal axis. This situation simulates real condition where the crack angle is unknown. The result of this test, i.e. the 2X amplitude variation versus β is shown in Fig. 9b. The crack angle can be deduced from this figure as to be either at 30° or 285° which is in agreement with the real crack that lies at 285° from the specified reference position exactly.

5 Conclusion

Coupled lateral and axial vibrations due to crack in a rotating shaft have been investigated experimentally for the purpose of crack detection. Auxiliary axial excitation is applied to the rotating shaft of the experimental rig. Horizontal and vertical responses are measured and analyzed for the uncracked and cracked conditions. Effects of changing crack-unbalance angle, running speed and crack depth are investigated. The following conclusions are drawn:

1. For the experiments conducted in this paper, the axial excitation frequency (f_i) and its harmonic ($2f_i$) are dominant in both horizontal and vertical lateral spectra which indicates coupling between axial and lateral vibration due to crack. However, for all studied cases, the horizontal spectra exhibit higher values compared with the vertical spectra.
2. The measured lateral vibration responses to the axial excitation are found to be sensitive to crack depth change. When the crack depth is increased from ($\bar{a} = 0.22$) to ($\bar{a} = 0.55$), the amplitude of the main crack feature (f_i) in horizontal direction has increased by 11 times. Therefore, crack growth can be effectively monitored using the auxiliary excitation method.
3. Increasing the running speed from 1/10th of the first critical speed of the rotor to 1/5th of the first critical speed helps in crack detection due to the appearance of the twice per revolution component ($2X$). In addition, the sum and difference frequencies appear around (f_i) and ($2f_i$) due to the interaction of the running frequency and its harmonics and the axial excitation frequency and its harmonics. Therefore, it is recommended to carry out the auxiliary excitation measurements at a running speed that equals one of the highest integer fractions of the first critical speed in the operating range of the machine as it will be the most informative. However, operating a cracked rotor that is subjected to an external force at very high speeds can be dangerous as it may cause crack propagation.
4. The crack-unbalance angle (β) greatly affects the horizontal and vertical responses to axial excitation. The pattern of (f_i) amplitude variation versus crack-unbalance angle depends upon the crack depth and the running speed of the rotor. On the other hand, the pattern of $2X$ amplitude variation is more general and can be used to specify the crack angle using trial mass test.

The main advantages of auxiliary excitation method are that it is an online method that can be used while the rotor is running; it is suitable for early crack detection; and the associated tests can be carried out by measurements on bearings or shafts. It is recommended to extend this work to study the effect of other common faults that may coexist with the crack in order to establish a robust method of crack detection based upon auxiliary excitation and coupling between vibrations.

Acknowledgment The first author wishes to gratefully thank Dr. Tamer El-Sayed for his technical support in assembling the experimental rig to achieve minimum fault condition.

References

1. Wauer J (1990) On the dynamics of cracked rotors: a literature survey. *Appl Mech Rev* 43:13–17
2. Gasch R (1983) A survey of the dynamic behavior of a simple rotating shaft with a transverse crack. *J Sound Vib* 160(2):313–332

3. Dimarogonas AD (1996) Vibration of cracked structure: a state of the art review. *Eng Fract Mech* 55(5):831–857
4. Sabnavis G, Kirk RG, Kasarda M, Quinn D (2004) Cracked shaft detection and diagnostics: a literature review. *Shock Vib Digest* 36(4):287–296
5. Kumar C, Rastogi V (2009) A brief review on dynamics of a cracked rotor. *Int J Rotating Mach* 2009:6, Article ID 758108
6. Papadopoulos CA, Dimarogonas AD (1987) Coupling of bending and torsional vibration of a cracked Timoshenko shaft. *Ing Arch* 57:257–266
7. Papadopoulos CA, Dimarogonas AD (1988) Coupled longitudinal and bending vibrations of a cracked shaft. *J Vib Acoust Stress Reliab Des* 110:1–8
8. Papadopoulos CA, Dimarogonas AD (1987) Coupled longitudinal and bending vibrations of a rotating shaft with an open crack. *J Sound Vib* 117(1):81–93
9. Papadopoulos CA, Dimarogonas AD (1988) Stability of cracked rotors in the coupled vibrations. *J Vib Acoust Stress Reliab Des* 110:356–359
10. Ostachowicz WM, Krawczuk M (1992) Coupled torsional and bending vibrations of a rotor with an open crack. *Arch Appl Mech* 62:191–201
11. Darpe AK, Gupta K, Chawla A (2002) Analysis of the response of a cracked Jeffcott rotor to axial excitation. *J Sound Vib* 249:429–445
12. Darpe AK, Gupta K, Chawla A (2003) Experimental investigations of the response of a cracked rotor to axial excitation. *J Sound Vib* 260:265–286
13. Darpe AK, Gupta K, Chawla A (2004) Coupled bending, longitudinal and torsional vibrations of a cracked rotor. *J Sound Vib* 269(1–2):33–60
14. Darpe AK, Gupta K, Chawla A (2004) Transient response and breathing behaviour of a cracked Jeffcott rotor. *J Sound Vib* 272:207–243
15. Sinou JJ (2009) Experimental response and vibrational characteristics of a slotted rotor. *Commun Nonlinear Sci Numer Simul* 14(7):3179–3194
16. Henry TA, Okah-Avae BE (1976) Vibrations in cracked shafts. In: *Vibrations in rotating machinery*. The Institution of Mechanical Engineers, Suffolk, pp 15–19
17. Mayes IW, Davies WGR (1976) The vibrational behaviour of a rotating shaft system containing a transverse crack. In: *Vibrations in rotating machinery*. The Institution of Mechanical Engineers, Suffolk, pp 53–65
18. Bachschmid N, Diana G, Pizzigoni B (1984) The influence of unbalance on cracked rotors. In: *Vibrations in rotating machinery*. Institution of Mechanical Engineers, Suffolk, pp 193–198
19. Sawicki JT, Wu X, Baaklini GY, Gyekenyesi AL (2003) Vibration-based crack diagnosis in rotating shafts during acceleration through resonance. In *NDE for Health Monitoring and Diagnostics*. International Society for Optics and Photonics, pp 1–10
20. Scheffer C, Girdhar P (2004) *Practical machinery vibration analysis and predictive maintenance*. Elsevier, Amsterdam